scientific reports

Check for updates

OPEN

Immunogenic cell death biomarkers for sepsis diagnosis and mechanism via integrated bioinformatics

Guansheng Li[1,4], Xiaoxing Tian[2,4], Enyao Wei[3], Feng Zhang[3] & Huang Liu[3]✉

Immunogenic cell death (ICD) has been implicated in sepsis, a condition with high mortality, through mechanisms involving endoplasmic reticulum stress and other pathophysiological pathways. This study aimed to identify and validate ICD-related biomarkers for sepsis diagnosis and to elucidate their underlying mechanisms. Publicly available datasets (GSE65682, GSE95233 and GSE69528) and 57 ICD-related genes (ICDRGs) were collected for analysis. Candidate genes were selected using differential expression analysis and weighted gene co-expression network analysis (WGCNA). By integrating machine learning models, receiver operating characteristic (ROC) curves, and gene expression analysis, biomarkers for sepsis diagnosis were identified. Gene set enrichment analysis (GSEA) and gene set variation analysis (GSVA) were conducted to explore the potential mechanisms by which the biomarkers influence sepsis. Additionally, immune infiltration analysis, subcellular localization, and disease association analysis were carried out. Finally, reverse transcription quantitative polymerase chain reaction (RT-qPCR) was used to validate the expression of the biomarkers in clinical sepsis blood samples. The biomarkers BCL2, PRF1, CXCR3, and EIF2AK3 demonstrated robust diagnostic potential for sepsis, each exhibiting an area under the curve (AUC) exceeding 0.8 in both the GSE65682 and GSE95233 datasets. These biomarkers were significantly downregulated in sepsis and were predominantly enriched in the ribosome. GSVA identified the top three activated pathways as β-alanine metabolism, citrate cycle/TCA cycle, and glyoxylate and dicarboxylate metabolism, while the most inhibited pathways included glycosphingolipid biosynthesis (lacto and neolacto series), α-linolenic acid metabolism, and linoleic acid metabolism. Immune infiltration analysis revealed reduced infiltration in sepsis, with CD8 + T cells showing the highest positive correlation with activated NK cells and PRF1. Subcellular localization analysis indicated that all four biomarkers were situated on the organelle membrane. Disease association analysis revealed correlations between these biomarkers and conditions such as hypertension and asthma. RT-qPCR analysis confirmed that the expression patterns of the biomarkers were consistent with the dataset findings, reinforcing the reliability and validity of the bioinformatic analyses. This study identified four ICD-related biomarkers (BCL2, PRF1, CXCR3, and EIF2AK3) that may help recognize early signs of sepsis, facilitate monitoring of disease progression, and have significant potential for clinical diagnosis and therapeutic strategies in sepsis.

Keywords Sepsis, Immunogenic cell death, Biomarkers, Machine learning, Immune infiltration analysis

Sepsis, characterized by life-threatening organ dysfunction, arises from a dysregulated host response to infection[1]. Sepsis and septic shock are increasingly prevalent, posing a substantial global health challenge due to their high morbidity and mortality rates[2,3]. Although the implementation of the Sequential Organ Failure Assessment (SOFA) and rapid SOFA scores has contributed to earlier diagnosis and a modest reduction in mortality, the overall mortality rate remains alarmingly high[4]. The Surviving Sepsis Campaign (SSC) guidelines primarily emphasize optimal supportive care, including hemodynamic management and the prevention of sepsis-related complications[5]. However, conventional therapeutic approaches fall short in addressing the aberrant immune

[1]Department of Critical Care Medicine, Chongqing Hospital of Traditional Chinese Medicine, Chongqing, China. [2]Department of Infectious Diseases, Renji Hospital, School of Medicine, Chongqing University, Chongqing, China. [3]Department of Respiratory and Critical Care Medicine, Chongqing Hospital of Traditional Chinese Medicine, Chongqing, China. [4]Guansheng Li and Xiaoxing Tian: Contributed equally to this work. [5]Guansheng Li and Xiaoxing Tian: Shared first authorship and author order was determined by drawing straws. ✉email: liuhuang01@sina.cn

activation and uncontrolled inflammatory responses that constitute the core pathophysiological mechanism of sepsis. Consequently, there is an urgent need to investigate the underlying pathogenesis and identify biomarkers that can facilitate early diagnosis, targeted treatment, and prognosis evaluation.

Immunogenic cell death (ICD), a distinct subtype of regulated cell death (RCD), occurs in infected or malignant cells, eliciting a specific immune response and generating immunological memory against antigens from dying cells[6]. ICD contributes to significant tissue damage in various pathological conditions, including sepsis[7]. Mechanistically, ICD is predominantly driven by endoplasmic reticulum (ER) stress[8,9], which acts synergistically with reactive oxygen species (ROS) to promote the surface exposure or release of damage-associated molecular patterns. These molecular signals stimulate immune cells to produce pro-inflammatory cytokines and chemokines, leading to tissue inflammation and damage during sepsis[10,11]. Given the complexity of sepsis pathogenesis, ER stress emerges as a pivotal pathological process[12,13], while immune suppression remains a hallmark of sepsis progression[14]. This evidence highlights the potential role of ICD in the onset and progression of sepsis, although the precise regulatory mechanisms remain insufficiently understood and warrant further elucidation. Critically, ICD-related genes serve as key regulators of programmed cell death mechanisms, while potentially modulating immune homeostasis and inflammatory cascades in the pathogenesis of sepsis. Therefore, the study of ICD-related genes may help to elucidate the mechanisms of ER stress and ROS generation in sepsis and provide new theoretical basis and potential therapeutic targets for early diagnosis and targeted therapy of sepsis.

This study employed differential expression analysis, weighted gene co-expression network analysis (WGCNA), machine learning, and other bioinformatics techniques to identify ICD-related biomarkers associated with sepsis. To elucidate the potential mechanisms and biological functions of these biomarkers, functional enrichment, subcellular localization, immune infiltration analysis, and regulatory network construction were performed. The findings aim to provide novel insights and a theoretical foundation for advancing sepsis diagnosis and therapeutic strategies.

Materials and methods

Data resource

Three sepsis datasets, GSE65682, GSE95233, and GSE69528 were retrieved from the Gene Expression Omnibus (GEO, https://www.ncbi.nlm.nih.gov/geo) platform. The GSE65682 dataset (platform: GPL13667) comprises whole blood samples from 760 patients with sepsis and 42 healthy donors. The GSE95233 dataset (platform: GPL570) includes whole blood samples from 51 patients with septic shock and 22 healthy donors. And the GSE69528 dataset (platform: GPL10558) includes whole blood samples from 83 patients with sepsis and 25 healthy donors. Detailed information on the three datasets can be found in Table S1. Additionally, 57 immunogenic cell death-related genes (ICDRGs) were obtained from public literature[15] (Table S2). The flow chart of this study is shown in Fig. S1. The codes for this study has been made available on GitHub [https://github.com/liuhu007/PCR/blob/20c8eed7f9e6f6d55af50a10a9ed6d89b7423b8d/Raw%20data.R].

Selection of differentially expressed genes (DEGs)

First, the data was normalized by the normalizeBetweenArrays function of the R package 'limma' (Ver. 3.54.0)[16]. In the GSE65682 dataset, differential expression analysis was conducted using the R package 'limma' (Ver. 3.54.0)[16], identifying DEGs between disease and control groups under the conditions of |log2fold change (FC)|> 0.5 and p-value < 0.05. Multiple corrections by the Benjamini-Hochberg (BH) method. DEGs were visualized using a volcano plot generated by the R package 'ggplot2' (Ver. 3.4.1)[17], and a heat map depicting the top 10 upregulated and downregulated DEGs was produced using the R package 'Pheatmap' (Ver. 1.0.12)[18]. Additionally, the expression matrix from GSE65682 was read to obtain genes and samples, lowly expressed genes were filtered out, a log transformation was performed, and PCA analysis was conducted to display the distribution of samples. The results were visualized using ggplot2 (Version 3.5.1) and Ggforce (Version 0.4.2).

Weighted gene co-expression network analysis (WGCNA)

WGCNA was performed to identify trait-associated target genes by evaluating correlations between gene modules and clinical traits. WGCNA was executed using the R package 'WGCNA' (Ver. 1.71)[19]. To assess sample correlation in the GSE65682 dataset, clustering analysis was initially performed to detect potential outliers. To ensure optimal consistency with a scale-free network topology, the scale-free topology model fit (R^2) was set to approximately 0.85, and the mean connectivity was leveled to 0, determining the optimal soft-thresholding power. Based on the hybrid dynamic tree-cutting standard, genes were clustered into distinct modules (minModuleSize = 30), and highly similar modules were merged when the module dissimilarity threshold (MEDissThres) was set to 0.3. Modules with |cor|> 0.3 and $p < 0.05$ were designated as key modules associated with sepsis, and genes within these key modules were consolidated to identify key module genes. Module membership was analyzed by generating a heatmap of the correlation of each gene with the module signature genes using the R package 'Pheatmap' (Ver. 1.0.12). Gene significance was performed based on modules significantly associated with sepsis (p value < 0.05 and correlation coefficient > 0.5) as key modules, and the correlation of each gene with the clinical feature (sepsis) was calculated. Pivotal genes were identified by combining module membership and gene importance.

Acquisition and functional exploration of candidate genes

Candidate genes were obtained by intersecting DEGs, key module genes, and ICDRGs using the R package 'ggVennDiagram' (Ver. 1.2.2)[20]. To explore the biological functions and pathways associated with candidate genes, Gene Ontology (GO) and Kyoto Encyclopedia of Genes and Genomes (KEGG)[21–23] enrichment analyses were performed using the R package 'clusterProfiler' (Ver. 4.7.1.003)[24] with the criterion adj.$p < 0.05$. The

background gene set for GO and KEGG enrichment analysis was the GSE65682 dataset. The top ten GO terms and the top five KEGG pathways were visualized using the 'clusterProfiler' and 'org.Hs.eg.db' package (Ver 3.18.0). Additionally, a protein–protein interaction (PPI) network was constructed using the Search Tool for the Retrieval of Interacting Genes/Proteins (STRING, https://string-db.org/) database with a confidence score of 0.4 and visualized using Cytoscape software (Ver. 3.9.1)[25] to investigate protein-level interactions among candidate genes.

Biomarkers screening for sepsis diagnosis

Based on the GSE65682 dataset, three machine learning (ML) models were constructed to identify feature genes associated with sepsis. These models included random forest (RF), support vector machine (SVM), and generalized linear model (GLM). The RF model was developed using the R package 'randomForest' (Ver. 4.7-1.1)[26], support vector machine (SVM) developed by R packages 'randomForest' (Ver. 4.7-1.1)[26], while the SVM model was also established using the same package. The GLM model was similarly constructed. To determine the most accurate model, performance evaluation was conducted using the R package 'DALEX' (Ver. 4.4.4)[27], calculating both the standardized root mean square residual (SRMR) and root mean square error (RMSE). The model exhibiting the lowest SRMR and RMSE was selected as the optimal model, and the genes identified within it were considered feature genes. To evaluate the diagnostic accuracy of these feature genes in sepsis, receiver operating characteristic (ROC) curves were generated for each gene using the 'pROC' package in R (Ver. 1.18.0)[28] for both GSE65682 and GSE95233 datasets. Genes with an area under the curve (AUC) exceeding 0.7 were classified as candidate biomarkers with significant diagnostic capability. Subsequently, gene expression analysis of these candidate biomarkers was performed in both datasets. The Wilcoxon rank-sum test was applied to compare the expression levels between the disease and control groups. Biomarkers demonstrating statistically significant differential expression ($p < 0.05$) in both datasets and consistent expression trends across the two groups were identified as validated biomarkers. Next, the identified biomarkers were validated one more time in the GSE69528 dataset using the same methodology. Additionally, Spearman's correlation analysis was conducted within the GSE65682 dataset to investigate the associations between these biomarkers ($p < 0.05$), and correlation heatmaps were drawn using pheatmap (Ver 1.0.12).

Functional analyses of biomarkers

To explore the functional roles of the identified biomarkers, gene set enrichment analysis (GSEA) was performed using the 'clusterProfiler' package in R. Pearson's correlation analysis was first conducted between each biomarker and other genes in the GSE65682 dataset to calculate correlation coefficients. The genes were then ranked according to their correlation coefficients, forming a sorted gene list for GSEA. The analysis utilized the background gene set (c2.cp.kegg.v2023.1.Hs.symbols) obtained from the Molecular Signatures Database (MSigDB, https://www.gsea-msigdb.org/gsea/msigdb/index.jsp) (adj.$p < 0.05$).

To investigate pathway alterations between the sepsis and control groups, gene set variation analysis (GSVA) was conducted using the R package 'GSVA' (Ver. 1.46.0)[29]. Single-sample GSEA (ssGSEA) scores for each pathway were calculated based on the reference gene set (C2: KEGG gene sets) from MSigDB, and differences in ssGSEA scores between the groups were statistically analyzed (adj.$p < 0.05$). The top five KEGG pathways with significant enrichment differences were visualized.

To identify genes functionally related to biomarkers, a gene–gene interaction (GGI) network was constructed using the GeneMANIA platform (http://genemania.org/). This network revealed the interactions between biomarkers and functionally related genes.

Immunoinfiltration analysis and drug prediction

To investigate the immune microenvironment landscape in sepsis, the CIBERSORT algorithm was applied to estimate the abundance of 22 immune cell types in the GSE65682 dataset. Samples with a p-value greater than 0.05 were excluded to ensure reliability. Differentially infiltrated immune cells between the disease and control groups were identified using the Wilcoxon rank-sum test, with a significance threshold of $p < 0.05$. Additionally, correlations between the 22 immune cell types and between immune cells and biomarkers were analyzed using Spearman's correlation method via the 'cor' function, with statistical significance set at $p < 0.05$.

To identify potential therapeutic compounds for sepsis, biomarkers were queried in the Drug-Gene Interaction Database (DGIdb, http://dgidb.org/). Predicted drug candidates targeting the biomarkers were compiled, and the interactions were visualized using a drug-biomarker interaction network generated by Cytoscape software.

Subcellular localization and association analysis of biomarkers with immune system or cardiovascular diseases

Subcellular localization analysis was performed to gain insights into the functional roles of biomarkers and their involvement in cellular processes and disease mechanisms. Biomarker protein localization within major organelles was predicted using the UniProt database (https://www.uniprot.org/), which encompasses comprehensive protein sequences and functional annotations.

To explore the association between biomarkers and typical immune system or cardiovascular diseases, the Comparative Toxicogenomics Database (CTD, http://ctdbase.org/) was utilized. The strength of associations was assessed by calculating inference scores, and the top five diseases, ranked by the highest inference scores, were selected for presentation.

Construction of biomarker-related regulatory networks

To elucidate the regulatory mechanisms underlying biomarker expression, upstream molecules were identified through a series of bioinformatic predictions. Initially, miRNAs targeting the biomarker were predicted using the

Transcription Antagonizing RNA Database (taRBase, http://www.microrna.gr/tarbase). The top ten miRNAs, selected based on the highest interaction degree and closest nodes, were subsequently utilized to predict lncRNAs via the miRNet platform (https://www.mirnet.ca/miRNet/home.xhtml). The lncRNA-miRNA-biomarker regulatory network was then constructed using Cytoscape software.

Furthermore, transcription factor (TF) prediction was conducted employing databases from the National Center for Biotechnology Information (NCBI, https://www.ncbi.nlm.nih.gov/), JASPAR (https://jaspar.elixir.no/), and the University of California Santa Cruz (UCSC, http://genome.ucsc.edu/). Specifically, the NCBI platform was used to extract promoter sequences, comprising 2000 bp upstream and 100 bp downstream nucleobase regions relative to biomarkers, based on the genome hg38 assembly. Subsequently, the JASPAR and UCSC databases were applied to predict TFs regulating biomarkers and to identify potential binding sites, respectively.

Reverse transcription-quantitative polymerase chain reaction (RT-qPCR)

To validate biomarker expression levels in clinical samples, RT-qPCR was conducted using 10 freshly collected blood samples. A 3 ml sepsis blood sample and PBMC separation liquid were introduced into 15 ml centrifuge tubes, followed by centrifugation at 2000 g for 20 min to isolate PBMCs. The PBMC layer was carefully transferred to a new centrifuge tube, supplemented with PBS to a final volume of 15 ml, and the cells were resuspended. Subsequent centrifugation at 1000 g for 10 min was performed, after which the supernatant was discarded. TRIzol (Ambion, USA) (1 ml) was then added at room temperature for 10 min to resuspend and lyse the cells. Chloroform (300 µl) was added, mixed vigorously for 30 s, and incubated at room temperature for 10 min to facilitate phase separation, followed by centrifugation at 12000 g and 4 °C for 15 min to stratify RNA. The aqueous phase was combined with an equal volume of ice-cold isopropyl alcohol (Chronchem, China) and centrifuged at 12000 g and 4 °C for 10 min to precipitate RNA. The resulting RNA pellet was washed with 1 ml of 75% ethanol (Chronchem, China), inverted for 2 min, and centrifuged at 7500 g and 4 °C for 5 min, with the washing process repeated twice. The RNA pellet was subsequently air-dried and dissolved in RNase-free water (Servicebio, China), and RNA concentration was measured. Reverse transcription of mRNA was performed using the SureScript First-Strand cDNA Synthesis Kit (Servicebio, China). Reagents and solutions (Table S3) were sequentially added on ice, followed by brief centrifugation. Reverse transcription was carried out using a PCR apparatus (BIO-RAD, USA) under the following conditions: 25 °C for 5 min, 50 °C for 15 min, 85 °C for 5 s, and hold at 4 °C. The cDNA product was diluted 5–20 times with ddH2O (RNase/DNase-free). Subsequent qPCR was conducted following the specified reaction system (Table S4) with the CFX96 real-time quantitative fluorescent PCR instrument (BIO-RAD, USA). Amplification involved 40 cycles comprising pre-denaturation at 95 °C for 1 min, denaturation at 25 °C for 2 min, annealing at 55 °C for 20 s, and extension at 72 °C for 30 s. Primer sequences (Tsingke, China) are detailed in Table S5. Amplification and melting curves were generated, and Ct values were recorded.

Statistical analysis

Bioinformatics analyses were performed using the R software (version 4.2.2), employing the Wilcoxon rank-sum test to assess inter-group differences, with statistical significance established at $p < 0.05$.

Results

A total of 3983 DEGs were screened

The distribution of the samples is shown in Fig. S2A and B. Following differential expression analysis, 3983 DEGs were identified, comprising 1269 upregulated and 2716 downregulated DEGs in the disease group of the GSE65682 dataset (Fig. 1A and B, Tables S6 and S7).

A total of 3177 key module genes were screened

Sample clustering analysis revealed an outlier (GSM1692250) within the GSE65682 dataset, which was excluded to maintain analytical accuracy (Fig. 1C). The soft threshold was established at 9 when R^2 approximated 0.85 and mean connectivity approached 0 (Fig. 1D). Gene classification yielded 40 modules by setting the minimum gene count per module to 30, which were subsequently merged into 17 similar modules (Fig. 1E). The list of genes corresponding to each module is shown in Table S8. Among these, the MEdarkgrey ($cor = -0.58$, $p = 1.0 \times 10^{-17}$), MEpaleturquoise ($cor = -0.54$, $p = 4.0 \times 10^{-61}$), and MEmagenta ($cor = 0.36$, $p = 5 \times 10^{-26}$) modules were identified as key modules (Fig. 1F). Integration of genes from these three modules resulted in a total of 3,177 key module genes. After calculating the correlation between each gene and the module characteristic genes, the top 10 modules with the strongest correlations were selected, along with the most correlated gene in each module. It was found that MBP, DHRS4, AASDHPPT, MEF2C, STXBP3, COX6C, TTC17, FCRL3, RPL14, and LOC728622 made significant contributions to the definition of the modules (Fig. S3A). Based on the MEdarkgrey, MEpaleturquoise, and MEmagenta modules significantly associated with sepsis, the correlation between each gene and the clinical feature (sepsis) was calculated. The top 10 genes with the highest correlations were KRTCAP2, MRPS18C, ZC3H15, GLYR1, DPY30, DBI, ATP5C1, KIAA1143, and ACOT13, which showed significant relevance in clinical research on sepsis (Fig. S3B). By comprehensively considering the relationships among module members and gene importance, 50 hub genes were identified (Table S9).

Candidate genes might influence sepsis by apoptosis and autophagy pathways

The intersection of 3,990 DEGs, 3,177 key module genes, and 57 ICDRGs yielded six candidate genes: CXCR3, PRF1, BCL2, EIF2AK3, PPIA, and IL17RA (Fig. 2A). Functional enrichment analysis identified 91 GO terms associated with candidate genes, including 77 biological processes (BPs), 10 cellular components (CCs), and four molecular functions (MFs), such as the regulation of intrinsic apoptotic signaling pathway, intrinsic apoptotic signaling pathway, and regulation of apoptotic signaling pathway ($p.adjust < 0.05$) (Fig. 2B, Table S2).

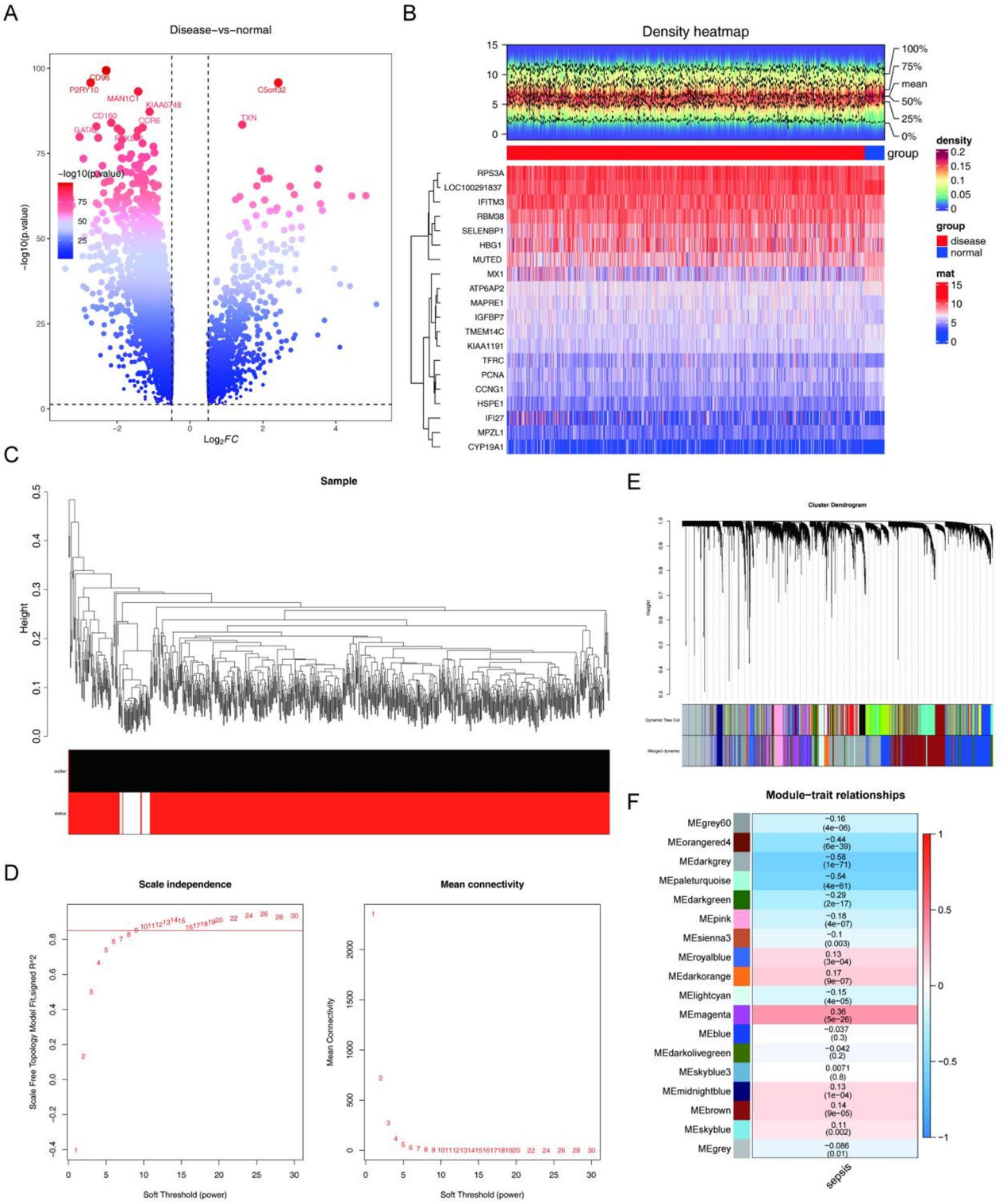

Fig. 1. Identification of differentially expressed genes (DEGs) and acquisition of the sepsis module genes. (**A–B**) Volcano and heat maps of differential genes in diseased and normal samples in the training set (**C**) Sample clustering analysis of GSE65682 dataset. (**D**) No-scale soft threshold distribution, the power threshold was set at 9. (**E**) The constructed co-expression network was clustered into 17 gene modules. (**F**) Heatmap showing the correlation of the modules and sepsis. Darkgrey, paleturquoise and magenta were selected as key modules.

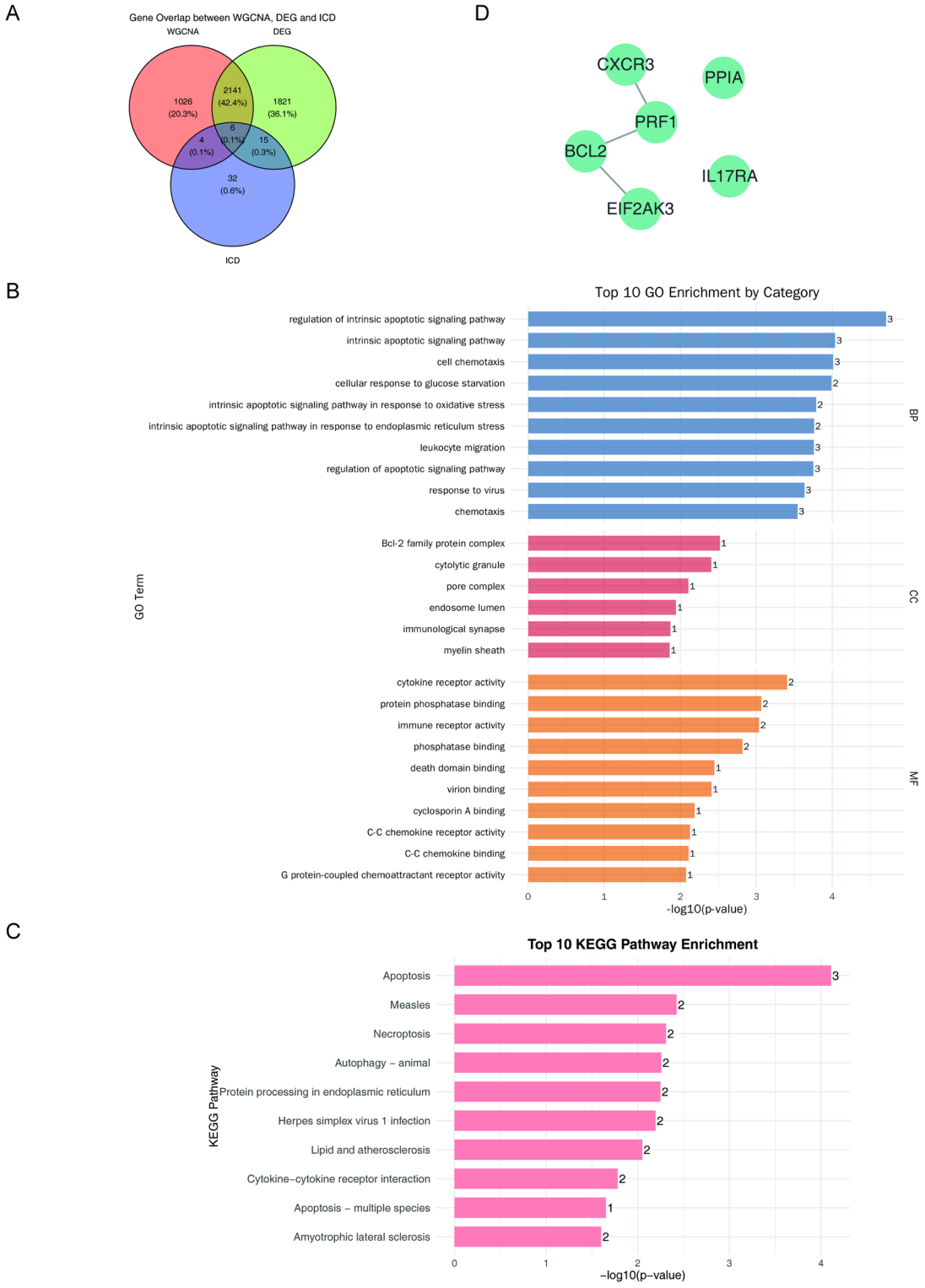

Fig. 2. Candidate genes might influence sepsis by apoptosis and autophagy pathways. (**A**)Venn diagram of DEGs, key module genes and ICDRGs intersecting genes. (**B**) The top ten items of GO enrichment analysis. (**C**) The top five pathways of KEGG enrichment analysis. (**D**) The PPI network of the six intersecting genes.

Additionally, candidate genes were involved in 107 KEGG pathways, notably including the apoptosis pathway (BCL2, PRF1, EIF2AK3) as well as autophagy-animal, measles, and protein processing in the endoplasmic reticulum (BCL2, EIF2AK3) ($p.adjust < 0.05$) (Fig. 2C, Table S2). Integrating GO and KEGG analyses indicated that candidate genes potentially modulate sepsis via apoptosis and autophagy pathways. The PPI network

demonstrated interactions among CXCR3, PRF1, BCL2, and EIF2AK3, while PPIA and IL17RA exhibited no interactions with other genes (Fig. 2D).

BCL2, PRF1, CXCR3, EIF2AK3, and PPIA were identified as biomarkers diagnosing sepsis

Machine learning techniques have emerged as effective strategies for gene screening. Among the three evaluated models, the RF model exhibited the lowest SRMR and RMSE values, indicating superior predictive performance with minimal error. Consequently, the RF model was selected as the optimal approach for identifying feature genes (Fig. 3A). Genes obtained from the RF model were ranked using the Mean Decrease Accuracy and Mean Decrease Gini methods, and the top five genes from both rankings were designated as feature genes: BCL2, PRF1, CXCR3, EIF2AK3, and PPIA (Fig. 3B). ROC curve analysis demonstrated that the AUC values of BCL2, PRF1, CXCR3, and EIF2AK3 exceeded 0.8 in both GSE65682 and GSE95233 datasets, indicating robust diagnostic efficacy for sepsis (Fig. 3C). These genes were identified as candidate biomarkers due to their significantly reduced expression levels in the disease groups of both datasets (Fig. 3D). In the GSE69528 dataset, BCL2, PRF1 and CXCR3 expression levels were significantly lower in the disease group (Fig. S4). Notably, Spearman's correlation analysis revealed positive correlations among the four biomarkers, except between CXCR3 and EIF2AK3. The strongest positive correlation was observed between BCL2 and EIF2AK3 ($cor = 0.42$, $p = 4.21 \times 10^{-34}$) (Fig. 3E). A heat map of the correlations between biomarkers is shown in Fig. S5.

Relevant functions biomarkers were revealed

GSEA indicated that all four biomarkers were significantly enriched in the ribosome pathway. Additionally, BCL2 and CXCR3 were implicated in primary immunodeficiency, while CXCR3 and PRF1 were associated with graft-versus-host disease (Fig. 4A, Table S2). Subsequent GSVA revealed 29 activated pathways and 21 inhibited pathways in the disease group. The top three upregulated pathways were β-alanine metabolism, citrate cycle/TCA cycle, and glyoxylate and dicarboxylate metabolism, while the most significantly downregulated pathways included glycosphingolipid biosynthesis (lacto and neolacto series), α-linolenic acid metabolism, and linoleic acid metabolism (Fig. 4B, Table S2). GeneMANIA analysis further identified functionally related genes, highlighting EIF2AK3 and BCL2 as closely interacting with BAX via the regulation of intrinsic apoptotic signaling pathways. Moreover, the biomarkers were linked to cellular calcium ion homeostasis and cytotoxicity against foreign cells (Fig. 4C).

Lowly infiltrated in sepsis, CD8 + T cells exhibited the highest positive correlations with activated NK cells and PRF1

The abundance of 22 immune cell types was visualized through a heatmap (Fig. 5A). Among the 18 differentially infiltrated immune cells, hyperinfiltration was observed in activated dendritic cells (DCs), monocytes, neutrophils, plasma cells, activated CD4 + memory T cells, and gamma delta (γδ) T cells, whereas naive B cells, resting DCs, M0 macrophages, activated natural killer (NK) cells, resting NK cells, naive CD4 + T cells, CD8 + T cells, and regulatory T cells (Tregs) exhibited reduced infiltration in the disease group ($p < 0.05$) (Fig. 5B). Correlation analysis revealed that activated mast cells had the strongest negative relationship with resting mast cells ($cor = -0.660$, $p < 0.001$), while activated NK cells demonstrated the most positive correlation with CD8 + T cells ($cor = 0.550$, $p < 0.001$) (Fig. 5C). Further exploration of the relationships between immune cells and biomarkers identified PRF1 as exhibiting the strongest positive correlation with CD8 + T cells ($cor = 0.504$, $p < 0.001$) and the most negative correlation with M0 macrophages ($cor = -0.277$, $p < 0.001$) (Fig. 5D). Drug-Gene Interaction Database (DGIdb) analysis predicted 79 compounds associated with the identified biomarkers. The drug-biomarker interaction network indicated that 76 compounds targeted BCL2, including CA4P, tretinoin, and selenium. In addition, IL-2 and emapalumab-lzsg were identified as interacting with PRF1, while GSK2606414 was the sole compound targeting EIF2AK3. Notably, no compounds were predicted to target CXCR3 (Fig. 5E).

Deciphering biomarker function through subcellular localization and disease association analysis

The subcellular localization of proteins encoded by biomarkers provides valuable insights into their functional roles. BCL2 was localized to the mitochondrial outer membrane, nuclear membrane, endoplasmic reticulum membrane, and cytoplasm, whereas PRF1 was detected in the cytosolic granule, secreted form, plasma membrane, and endosomal lumen. CXCR3 and EIF2AK3 were individually localized to the cell membrane and endoplasmic reticulum membrane, respectively (Fig. 6A). Disease association analysis identified the top five immune system and cardiovascular diseases related to the biomarkers, with hypertension and asthma exhibiting the strongest associations (Fig. 6B).

The expression of biomarkers was regulated by upstream molecules

To elucidate the regulatory mechanisms of biomarkers, 125 miRNAs regulating the four biomarkers were identified using the taRBase database. Additionally, the 10 lncRNAs with the highest interaction degrees with these miRNAs were selected to construct the lncRNA-miRNA-biomarker network (Table S2). As illustrated in Fig. 6C, Myd88 was predicted to be regulated by hsa-mir-429, hsa-mir-155-5p, and hsa-mir-21-5p. The lncRNA XIST was implicated in regulating hsa-mir-124-3p, potentially affecting PRF1 expression. Furthermore, TFs modulating CXCR3 and PRF1 were identified, indicating that both biomarkers are co-regulated by FOXO1 (Fig. 6D and E). No TFs were predicted for BCL2 and EIF2AK3.

RT-qPCR results

RT-qPCR validation demonstrated that three biomarkers (PRF1, CXCR3, and EIF2AK3) exhibited significantly reduced expression levels in sepsis samples compared to control samples, while BCL2 also displayed low

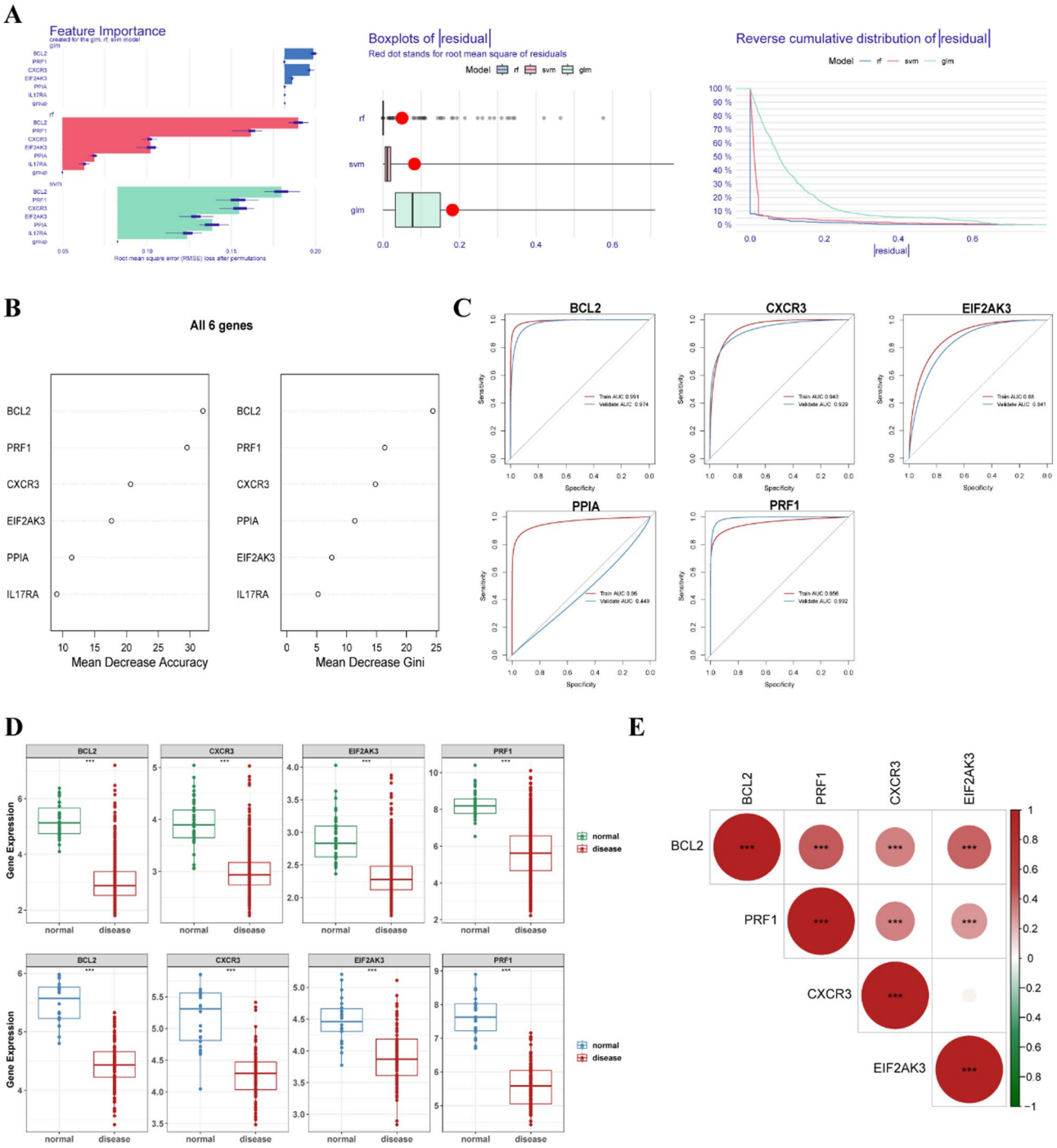

Fig. 3. BCL2, PRF1, CXCR3, EIF2AK3 and PPIA were identified as biomarkers diagnosing sepsis. (**A**) Model screening chart. The left shows the feature importance of models, the right shows reverse cumulative distribution of residual, the middle is boxplots of residual. (**B**) The top five feature genes obtained by RF analysis. (**C**) ROC plots of the diagnostic performance of the candidate biomarkers. The red is the ROC curve in the training set, and the blue is the ROC curve in the validation set. (**D**) Expression analysis of four candidate biomarkers. The top is the expression in the training set, and the bottom is the expression in the validation set. (**E**) Heatmap showing the associations among the biomarkers.

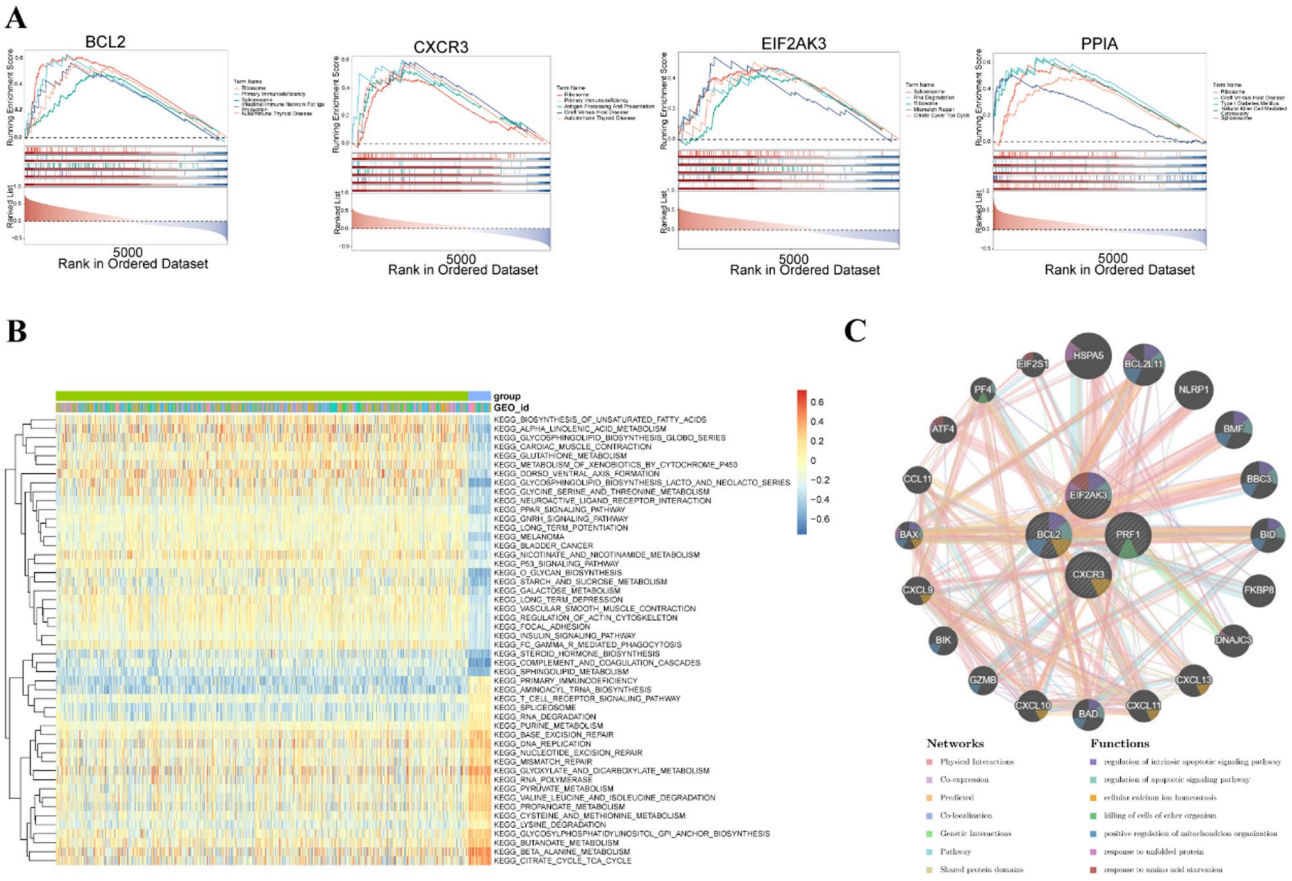

Fig. 4. Functional analyses of four biomarkers. (**A**) The TOP5 functional pathways of the biomarkers by GSEA. (**B**) The GSVA scores in the disease vs normal group. (**C**) GGI network showing the interaction of biomarkers and functionally related genes.

expression in sepsis samples but without statistical significance (Fig. 7A and D). These results align with the expression trends observed in the database, affirming the robustness and clinical relevance of the analysis results.

Discussion

Sepsis poses a significant threat to human health and remains a prevalent condition with high mortality rates despite advancements in clinical recognition and diagnostic practices. Current therapeutic approaches are primarily limited to organ support and fluid resuscitation, underscoring the urgent need to identify key biomarkers to elucidate sepsis pathogenesis and mitigate mortality[4]. In this study, bioinformatic analysis of patients with sepsis from the GEO database identified BCL2, PRF1, CXCR3, and EIF2AK3 as ICD-related biomarkers. All four biomarkers exhibited significant enrichment in ribosomal pathways, and RT-qPCR expression trends in clinical samples mirrored those observed in the datasets. These findings offer new insights into the early diagnosis and therapeutic strategies for sepsis.

BCL2 functions as an apoptosis inhibitor and also impedes autophagy, with its protein predominantly localized to the nuclear membrane, endoplasmic reticulum membrane, and mitochondrial outer membrane[30,31]. Autophagy has been implicated in the pathophysiological mechanisms of sepsis, and among autophagy-related biomarkers, BCL2 demonstrates notable diagnostic potential[32]. Consequently, BCL2 may attenuate sepsis progression through the inhibition of autophagy and apoptosis. Moreover, downregulation of BCL2 has been associated with exacerbation of LPS-induced myocardial injury in septic mice, suggesting its potential protective role in sepsis[33].

PRF1, a cytotoxic protein predominantly expressed in cytotoxic T lymphocytes (CTLs) and NK cells, is integral to the immune response through a granule-dependent cytolytic pathway, facilitating the elimination of infected or malignant host cells[34]. Evidence indicates that PRF1 expression is significantly reduced in sepsis and positively correlates with prognosis[35,36]. Consistent with previous studies, both dataset analysis and RT-qPCR validation in the current study confirmed a marked decrease in PRF1 expression in sepsis. This finding implies that PRF1 contributes to the immune response in sepsis by enhancing pathogen clearance via CTLs and NK cells.

CXCR3, a chemokine receptor of the CXC subfamily, is predominantly expressed on the outer plasma membrane surface of activated T cells, B cells, and NK cells, mediating targeted migration and immune responses through receptor-ligand interactions on target cell membranes. CXCR3 plays a critical role in autoimmune diseases, infections, and tumor immunity[37,38]. Previous studies have demonstrated that migration of CXCR3 + T

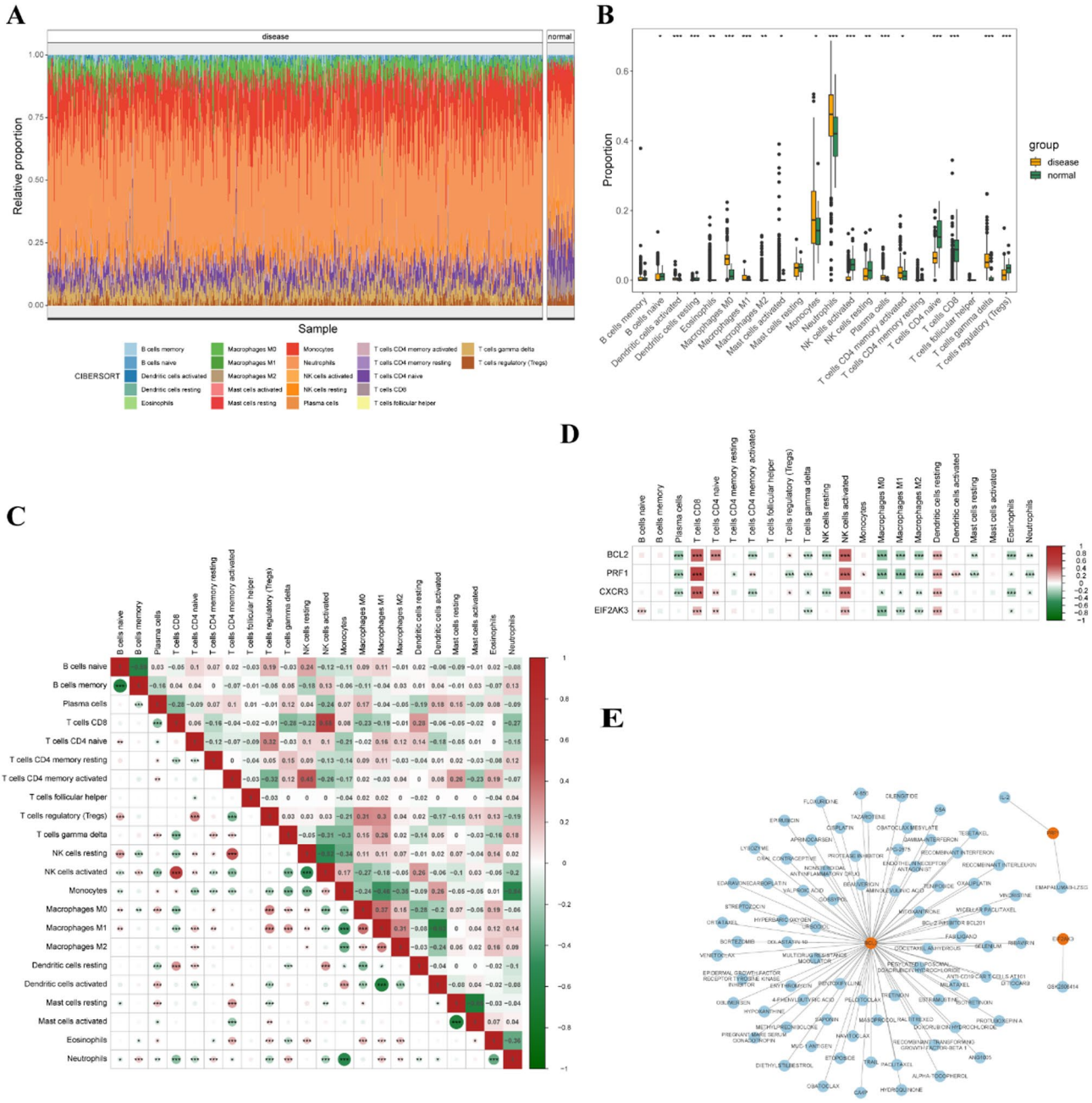

Fig. 5. Results of immunoinfiltration analysis and drug prediction. (**A**) Heatmap showing the abundance of 22 immune cell types. (**B**) The boxplot shows 18 differentially infiltrated immune cells between disease and controls. $*p < 0.05$, $**p < 0.01$, $***p < 0.001$. (**C**) Heatmap showing the correlation of 22 immune cells. (**D**) Heatmap showing the correlation between biomarkers and immune cells. (**E**) Drug-biomarker interaction network. Red circles as k biomarkers, blue circles as indicate drugs.

lymphocytes exacerbates sepsis-related lung injury[39], while CXCR3 blockade mitigates severe lung injury by reducing endothelial cell apoptosis[40]. Moreover, CXCR3 expression on CD4 + T cells has emerged as a potential marker for early sepsis detection[41,42]. Functional analysis in this study identified CXCR3 involvement in primary immunodeficiency and graft-versus-host disease, indicating its role in modulating immune responses and apoptosis during the early stages of sepsis.

EIF2AK3, also known as protein kinase RNA-like endoplasmic reticulum kinase (PERK), is a principal eIF2α kinase that plays a pivotal role during ER stress. Inflammatory responses that induce ER stress and disrupt ER functional homeostasis are closely associated with sepsis progression[43]. As a key gene linked to autophagy, EIF2AK3 demonstrates diagnostic efficacy for sepsis and correlates with patient prognosis[32], suggesting that EIF2AK3 may modulate sepsis progression through the regulation of ER stress and autophagy.

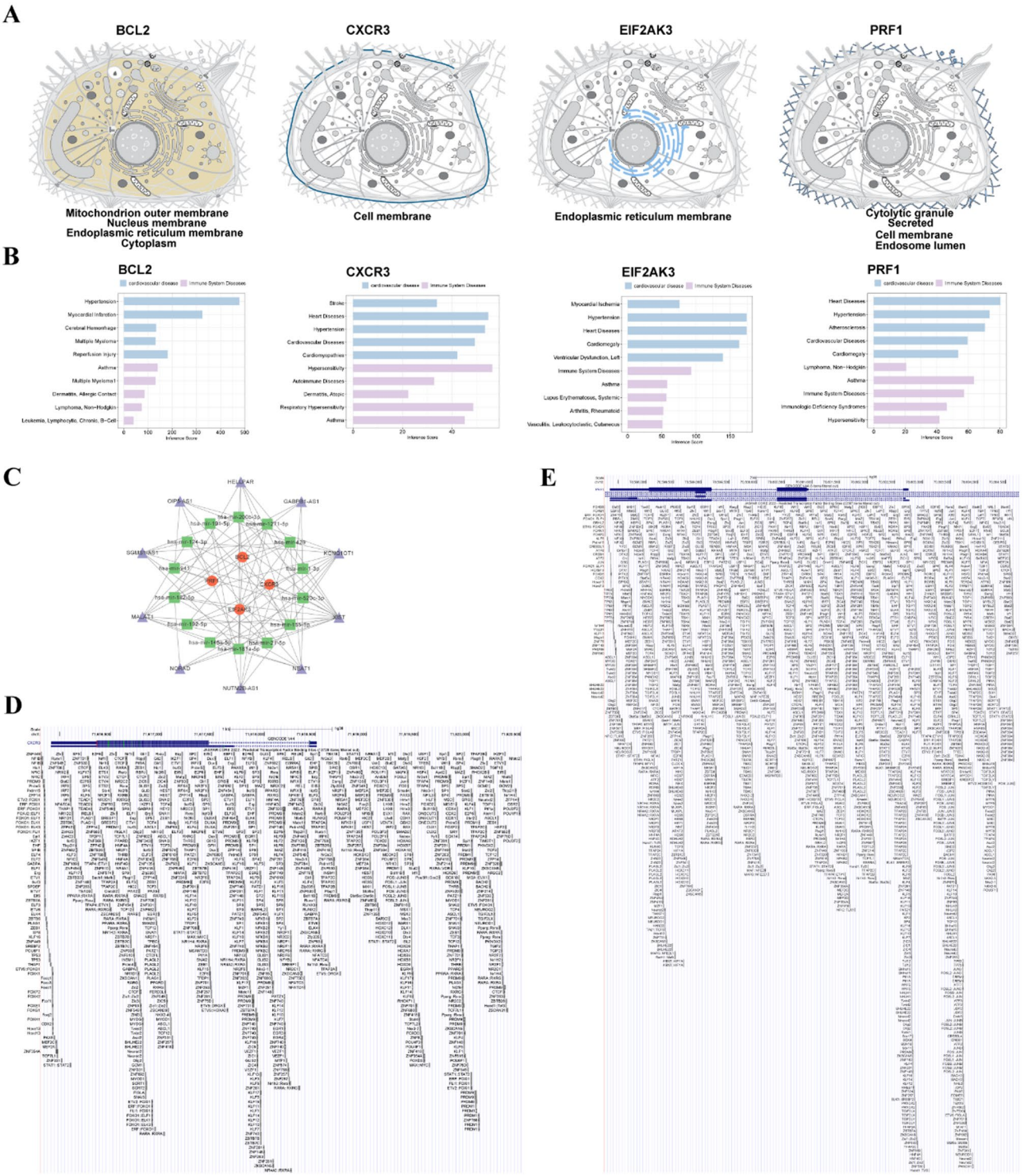

Fig. 6. The functions and related regulatory networks of biomarkers. (**A**) Subcellular localization of four biomarkers. (**B**) The top 5 immune system and cardiovascular diseases associated with bi.omarkers. (**C**) lncRNA-miRNA-biomarker network of biomarkers. (**D**) Transcription factors of CXCR3 and its potential binding sites. (**E**) Transcription factors of PRF1 and its potential binding sites.

Ribosomes function as essential molecular machinery for protein synthesis, underpinning cellular function by translating mRNAs into proteins[44]. In the context of sepsis, platelets have been shown to splice several pre-mRNAs into mRNAs, which are subsequently translated into proteins on ribosomes. These pre-mRNAs are susceptible to modulation by pathogens and bacterial products[45]. In this study, GSEA demonstrated that all four biomarkers (BCL2, PRF1, CXCR3, and EIF2AK3) were significantly enriched in ribosomes, suggesting that these

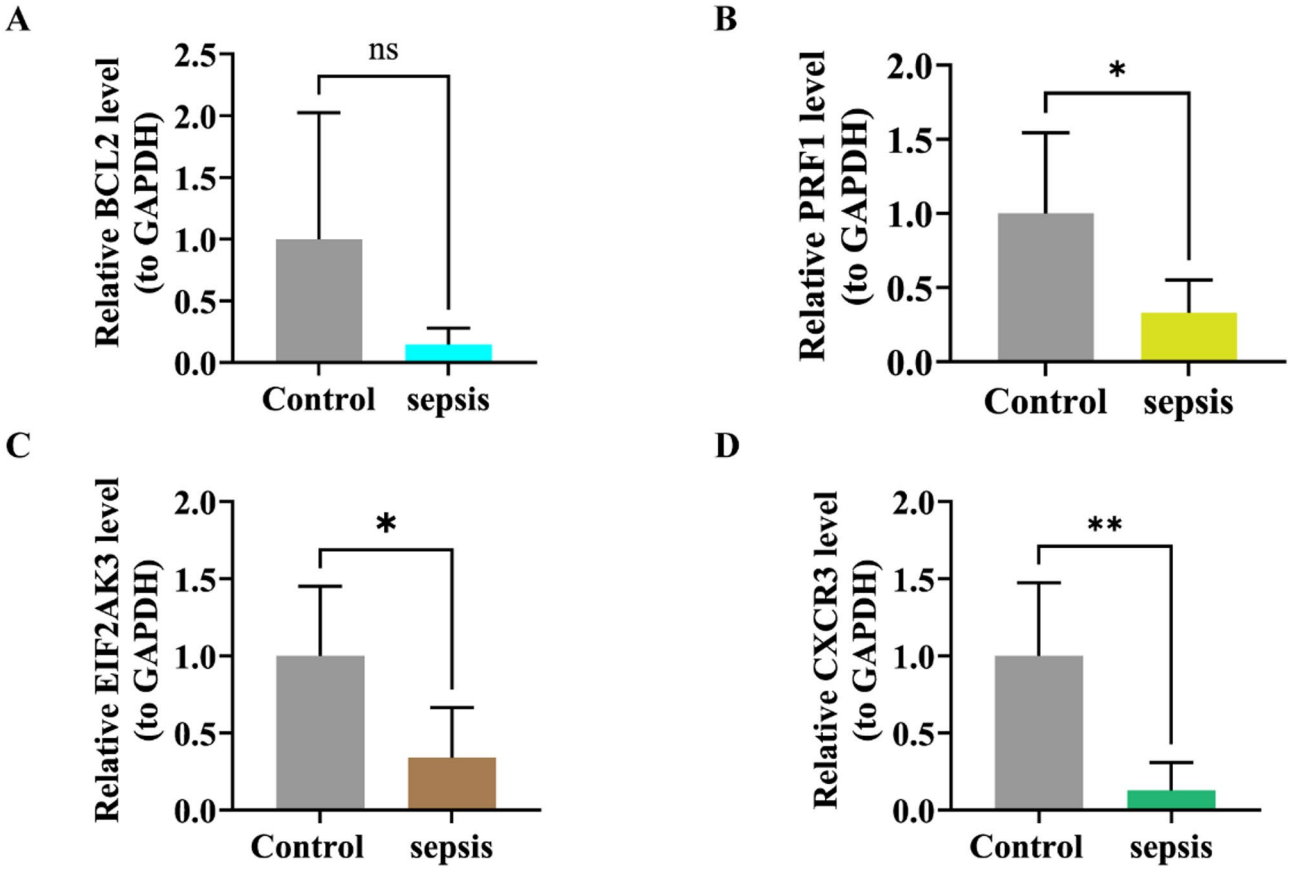

Fig. 7. RT-qPCR validation of biomarkers in clinical samples. *$p < 0.05$, **$p < 0.01$, ns indicates that the difference is not significant.

biomarkers may influence sepsis progression through ribosomal pathways. GSVA identified 29 activated and 21 inhibited pathways within the disease group. The most upregulated pathways included the β-alanine metabolism pathway, the tricarboxylic acid (TCA) cycle, and the glyoxylate and dicarboxylate metabolism pathway. The TCA cycle, a fundamental cellular metabolic pathway, not only plays a critical role in energy production but also exerts non-metabolic signaling effects. Its metabolites are involved in chromatin modification, DNA methylation, and post-translational protein modification, thereby regulating the immune response[46,47]. Remodeling of the TCA cycle and upregulation of mitochondrial genes associated with the TCA cycle have been shown to exert protective effects against sepsis[48,49]. BCL2 upregulation has been reported to maintain ROS at physiological levels without impairing TCA metabolism[50]. Sepsis frequently induces skeletal muscle atrophy, with the β-alanine metabolism pathway being significantly enriched in the gastrocnemius skeletal muscle affected by sepsis[51]. Increased BCL2 expression may modulate the β-alanine pathway, potentially affecting sepsis progression[52]. Additionally, the glyoxylate and dicarboxylate metabolism pathway has been implicated in bacterial biofilm formation[53] and may be involved in the pathogenesis of late-onset sepsis (LOS) in preterm infants[54]. Although the precise regulatory mechanisms by which these biomarkers influence the associated pathways remain unclear, it is postulated that PRF1 and CXCR3 may contribute to sepsis progression by enhancing the TCA cycle pathway, whereas EIF2AK3 might primarily regulate the glyoxylate and dicarboxylate metabolism pathway. Further experimental validation is necessary to substantiate these hypotheses.

Immune infiltration analysis revealed reduced infiltration of CD8 + T cells and M0 macrophages in sepsis. Previous studies have reported a decline in CD8 + T cell numbers and functional responses associated with sepsis[55]. Additionally, LPS-induced M0 macrophages have been shown to mitigate sepsis-induced myocardial injury by promoting M2 macrophage polarization[56]. The phenotype of CD8 + T cells has also been identified as a key factor in the early diagnosis of sepsis[57]. In the present study, PRF1 exhibited the strongest positive correlation with CD8 + T cells and the most pronounced negative correlation with M0 macrophages, suggesting that PRF1 may influence sepsis progression by modulating immune responses mediated by CD8 + T cells and M0 macrophages. Recent research on COVID-19 has highlighted the critical role of CD8 + T cells in maintaining a balanced immune response. Notably, PRF1 mRNA expression in CD8 + T cells was significantly elevated in patients with COVID-19 compared to healthy controls on day 5[58]. However, the expression dynamics of PRF1 in sepsis remain unclear, necessitating further experimental investigation.

Drug prediction analysis identified several compounds with potential therapeutic value in sepsis. Notably, IL-2 and emapalumab-lzsg were predicted to interact with PRF1. IL-2, a multifunctional cytokine essential

for Treg proliferation and survival within peripheral lymphoid tissues, is pivotal for modulating inflammatory responses and autoimmunity. Low-dose IL-2 therapy has demonstrated efficacy in treating autoimmune diseases[59,60]. Emapalumab, an IFN-γ-targeting monoclonal antibody, has been shown to be safe and effective in treating haemophagocytic lymphohistiocytosis (HLH)[61]. These findings suggest that targeting cytokine-mediated pathways could represent a promising strategy for managing immune dysregulation in sepsis. Given the involvement of multiple cytokines in immunogenic cell death, further exploration of these therapeutic targets is warranted. In preclinical studies, animal models of sepsis can be used to further investigate the mechanism of action of IL-2 and emapalumab-lzsg, optimise the therapeutic dose and provide data to support subsequent clinical trials. In future clinical trials, drug prediction analyses may be used to identify patients who are more likely to respond to IL-2 treatment and thus personalise the dose or combination regimen. In addition, emapalumab-lzsg may have greater efficacy in patients with immune disorders and severe inflammatory responses, and its therapeutic efficacy could be further evaluated in clinical trials.

In summary, the present study identified four ICD-related biomarkers (BCL2, PRF1, CXCR3, and EIF2AK3) that may influence sepsis progression via apoptosis and autophagy pathways, offering novel insights and potential strategies for sepsis diagnosis and treatment. However, this study has several limitations, primarily the lack of validation models based on basic experimental and clinical trials, which restricts the assessment of the clinical relevance and utility of these biomarkers. Secondly, the sample size selected for this study was limited due to time and resource constraints, which may affect the reliability and generalisability of the results. Therefore, future research should focus on collecting additional preclinical and clinical samples, constructing validation models, and conducting comprehensive analyses to establish the diagnostic, therapeutic, and prognostic potential of these biomarkers in sepsis. In addition, the analysis of immune cell infiltration may be influenced by patient clinical characteristics, genetic background, immune status and disease type. Future studies may be able to more accurately assess the relationship of immune cell infiltration by refining patient stratification criteria and using multivariate regression analysis or stratified analysis methods.

Data availability

The datasets analyzed for this study can be found in the [GEO] [https://www.ncbi.nlm.nih.gov/geo/].

Received: 23 February 2025; Accepted: 20 May 2025
Published online: 27 May 2025

References

1. Singer, M. et al. The third international consensus definitions for sepsis and septic shock (Sepsis-3). *JAMA* **315**, 801–810. https://doi.org/10.1001/jama.2016.0287 (2016).
2. Schlapbach, L. J. et al. International consensus criteria for pediatric sepsis and septic shock. *JAMA* **331**, 665–674. https://doi.org/10.1001/jama.2024.0179 (2024).
3. Chiu, C. & Legrand, M. Epidemiology of sepsis and septic shock. *Curr. Opin. Anaesthesiol.* **34**, 71–76. https://doi.org/10.1097/aco.0000000000000958 (2021).
4. Jang, J. H. et al. Navigating the modern landscape of sepsis: Advances in diagnosis and treatment. *Int. J. Mol. Sci.* https://doi.org/10.3390/ijms25137396 (2024).
5. Evans, L. et al. Surviving sepsis campaign: international guidelines for management of sepsis and septic shock 2021. *Intensive. Care. Med.* **47**, 1181–1247. https://doi.org/10.1007/s00134-021-06506-y (2021).
6. Galluzzi, L. et al. Consensus guidelines for the definition, detection and interpretation of immunogenic cell death. *J. Immunother. Cancer.* https://doi.org/10.1136/jitc-2019-000337 (2020).
7. Kolbrink, B. et al. TAT-RHIM: A more complex issue than expected. *Biochem. J.* **479**, 259–272. https://doi.org/10.1042/bcj20210677 (2022).
8. Chen, X., Shi, C., He, M., Xiong, S. & Xia, X. Endoplasmic reticulum stress: Molecular mechanism and therapeutic targets. *Signal. Transduct. Target. Ther.* **8**, 352. https://doi.org/10.1038/s41392-023-01570-w (2023).
9. Wang, J. et al. Endoplasmic reticulum-targeted delivery of celastrol and PD-L1 siRNA for reinforcing immunogenic cell death and potentiating cancer immunotherapy. *Acta. Pharm. Sin. B.* **14**, 3643–3660. https://doi.org/10.1016/j.apsb.2024.04.010 (2024).
10. Denning, N. L., Aziz, M., Gurien, S. D. & Wang, P. DAMPs and NETs in sepsis. *Front. Immunol.* **10**, 2536. https://doi.org/10.3389/fimmu.2019.02536 (2019).
11. Garg, A. D. et al. Molecular and translational classifications of DAMPs in immunogenic cell death. *Front. Immunol.* **6**, 588. https://doi.org/10.3389/fimmu.2015.00588 (2015).
12. Wallaeys, C. et al. Paneth cell TNF signaling induces gut bacterial translocation and sepsis. *Cell. Host. Microbe.* **32**, 1725-1743. e1727. https://doi.org/10.1016/j.chom.2024.08.007 (2024).
13. Sun, S. et al. Neutrophil extracellular traps impair intestinal barrier functions in sepsis by regulating TLR9-mediated endoplasmic reticulum stress pathway. *Cell. Death. Dis.* **12**, 606. https://doi.org/10.1038/s41419-021-03896-1 (2021).
14. Venet, F. & Monneret, G. Advances in the understanding and treatment of sepsis-induced immunosuppression. *Nat. Rev. Nephrol.* **14**, 121–137. https://doi.org/10.1038/nrneph.2017.165 (2018).
15. Wang, Z. et al. Identification of key biomarkers associated with immunogenic cell death and their regulatory mechanisms in severe acute pancreatitis based on WGCNA and machine learning. *Int. J. Mol. Sci.* https://doi.org/10.3390/ijms24033033 (2023).
16. Ritchie, M. E. et al. limma powers differential expression analyses for RNA-sequencing and microarray studies. *Nucleic. Acids. Res.* **43**, e47. https://doi.org/10.1093/nar/gkv007 (2015).
17. Liu, S., Xie, X., Lei, H., Zou, B. & Xie, L. Identification of key circRNAs/lncRNAs/miRNAs/mRNAs and pathways in preeclampsia using bioinformatics analysis. *Med. Sci. Monit.* **25**, 1679–1693. https://doi.org/10.12659/msm.912801 (2019).
18. Wang, Y. et al. Unveiling the key genes, environmental toxins, and drug exposures in modulating the severity of ulcerative colitis: a comprehensive analysis. *Front. Immunol.* **14**, 1162458. https://doi.org/10.3389/fimmu.2023.1162458 (2023).
19. Langfelder, P. & Horvath, S. WGCNA: an R package for weighted correlation network analysis. *BMC Bioinformatics* **9**, 559. https://doi.org/10.1186/1471-2105-9-559 (2008).
20. Gao, C. H., Yu, G. & Cai, P. ggVennDiagram: An intuitive, easy-to-use, and highly customizable R package to generate venn diagram. *Front. Genet.* **12**, 706907. https://doi.org/10.3389/fgene.2021.706907 (2021).
21. Kanehisa, M., Furumichi, M., Sato, Y., Matsuura, Y. & Ishiguro-Watanabe, M. KEGG: biological systems database as a model of the real world. *Nucleic Acids Res.* **53**, D672-d677. https://doi.org/10.1093/nar/gkae909 (2025).

22. Kanehisa, M. Toward understanding the origin and evolution of cellular organisms. *Protein Sci.* **28**, 1947–1951. https://doi.org/10.1002/pro.3715 (2019).
23. Kanehisa, M. & Goto, S. KEGG: Kyoto encyclopedia of genes and genomes. *Nucleic Acids Res.* **28**, 27–30. https://doi.org/10.1093/nar/28.1.27 (2000).
24. Yu, G., Wang, L. G., Han, Y. & He, Q. Y. clusterProfiler: An R package for comparing biological themes among gene clusters. *OMICS* **16**, 284–287. https://doi.org/10.1089/omi.2011.0118 (2012).
25. Chin, C. H. et al. cytoHubba: identifying hub objects and sub-networks from complex interactome. *BMC. Syst. Biol.* **8**(Suppl 4), S11. https://doi.org/10.1186/1752-0509-8-s4-s11 (2014).
26. Alderden, J. et al. Predicting pressure injury in critical care patients: A machine-learning model. *Am. J. Crit. Care.* **27**, 461–468. https://doi.org/10.4037/ajcc2018525 (2018).
27. Feng, S. et al. Prediction model for spinal cord injury in spinal tuberculosis patients using multiple machine learning algorithms: a multicentric study. *Sci. Rep.* **14**, 7691. https://doi.org/10.1038/s41598-024-56711-0 (2024).
28. Robin, X. et al. pROC: an open-source package for R and S+ to analyze and compare ROC curves. *BMC Bioinformatics* **12**, 77. https://doi.org/10.1186/1471-2105-12-77 (2011).
29. Hänzelmann, S., Castelo, R. & Guinney, J. GSVA: Gene set variation analysis for microarray and RNA-seq data. *BMC Bioinform.* **14**, 7. https://doi.org/10.1186/1471-2105-14-7 (2013).
30. Siddiqui, W. A., Ahad, A. & Ahsan, H. The mystery of BCL2 family: Bcl-2 proteins and apoptosis: an update. *Arch. Toxicol.* **89**, 289–317. https://doi.org/10.1007/s00204-014-1448-7 (2015).
31. Ashkenazi, A., Fairbrother, W. J., Leverson, J. D. & Souers, A. J. From basic apoptosis discoveries to advanced selective BCL-2 family inhibitors. *Nat. Rev. Drug. Discov.* **16**, 273–284. https://doi.org/10.1038/nrd.2016.253 (2017).
32. Yang, L. et al. Diagnostic and prognostic value of autophagy-related key genes in sepsis and potential correlation with immune cell signatures. *Front. Cell. Dev. Biol.* **11**, 1218379. https://doi.org/10.3389/fcell.2023.1218379 (2023).
33. Zhang, R. et al. LncRNA SNHG1 promotes sepsis-induced myocardial injury by inhibiting Bcl-2 expression via DNMT1. *J. Cell. Mol. Med.* **26**, 3648–3658. https://doi.org/10.1111/jcmm.17358 (2022).
34. Guan, X. et al. Perforin 1 in cancer: Mechanisms, therapy, and outlook. *Biomolecules* https://doi.org/10.3390/biom14080910 (2024).
35. Liang, G., Li, J., Pu, S. & He, Z. Screening of sepsis biomarkers based on bioinformatics data analysis. *J. Healthc. Eng.* **2022**, 6788569. https://doi.org/10.1155/2022/6788569 (2022).
36. Chen, G. et al. Screening of four lysosome-related genes in sepsis based on RNA sequencing technology. *BMC. Immunol.* **24**, 50. https://doi.org/10.1186/s12865-023-00588-7 (2023).
37. Lv, L. et al. Mannose inhibits plasmodium parasite growth and cerebral malaria development via regulation of host immune responses. *Front. Immunol.* **13**, 859228. https://doi.org/10.3389/fimmu.2022.859228 (2022).
38. Wang, X. et al. The role of CXCR3 and its ligands in cancer. *Front. Oncol.* **12**, 1022688. https://doi.org/10.3389/fonc.2022.1022688 (2022).
39. Wang, J. et al. Sustained induction of IP-10 by MRP8/14 via the IFNβ-IRF7 axis in macrophages exaggerates lung injury in endotoxemic mice. *Burns. Trauma.* **11**, tkad006. https://doi.org/10.1093/burnst/tkad006 (2023).
40. Zhu, X. et al. Blockade of CXC chemokine receptor 3 on endothelial cells protects against sepsis-induced acute lung injury. *J. Surg. Res.* **204**, 288–296. https://doi.org/10.1016/j.jss.2016.04.067 (2016).
41. Kealy, D. et al. Blood immune profiles reveal a CXCR3/CCR5 axis of dysregulation in early sepsis. *J. Leukoc. Biol.* https://doi.org/10.1093/jleuko/qiae204 (2024).
42. Burton, R. J. et al. Conventional and unconventional T-cell responses contribute to the prediction of clinical outcome and causative bacterial pathogen in sepsis patients. *Clin. Exp. Immunol.* **216**, 293–306. https://doi.org/10.1093/cei/uxae019 (2024).
43. Gong, T. et al. Identification of immune-related endoplasmic reticulum stress genes in sepsis using bioinformatics and machine learning. *Front. Immunol.* **13**, 995974. https://doi.org/10.3389/fimmu.2022.995974 (2022).
44. Breznak, S. M., Kotb, N. M. & Rangan, P. Dynamic regulation of ribosome levels and translation during development. *Semin. Cell. Dev. Biol.* **136**, 27–37. https://doi.org/10.1016/j.semcdb.2022.06.004 (2023).
45. Middleton, E. A. et al. Sepsis alters the transcriptional and translational landscape of human and murine platelets. *Blood* **134**, 911–923. https://doi.org/10.1182/blood.2019000067 (2019).
46. Abhimanyu, et al. TCA metabolism regulates DNA hypermethylation in LPS and Mycobacterium tuberculosis-induced immune tolerance. *Proc. Natl. Acad. Sci. USA* **121**, e2404841121. https://doi.org/10.1073/pnas.2404841121 (2024).
47. Martínez-Reyes, I. & Chandel, N. S. Mitochondrial TCA cycle metabolites control physiology and disease. *Nat. Commun.* **11**, 102. https://doi.org/10.1038/s41467-019-13668-3 (2020).
48. Zeng, Z. et al. The pyruvate dehydrogenase complex in sepsis: Metabolic regulation and targeted therapy. *Front. Nutr.* **8**, 783164. https://doi.org/10.3389/fnut.2021.783164 (2021).
49. Li, Y. et al. Songorine promotes cardiac mitochondrial biogenesis via Nrf2 induction during sepsis. *Redox. Biol.* **38**, 101771. https://doi.org/10.1016/j.redox.2020.101771 (2021).
50. Fan, T. et al. Metabolomic and transcriptomic profiling of hepatocellular carcinomas in Hras12V transgenic mice. *Cancer. Med.* **6**, 2370–2384. https://doi.org/10.1002/cam4.1177 (2017).
51. Ilaiwy, A. et al. Identification of metabolic changes in Ileum, Jejunum, Skeletal Muscle, Liver, and Lung in a continuous I.V. pseudomonas aeruginosa model of sepsis using nontargeted metabolomics analysis. *Am. J. Pathol.* **189**, 1797–1813. https://doi.org/10.1016/j.ajpath.2019.05.021 (2019).
52. Zhou, S. et al. Porcine cardiac blood - Salvia miltiorrhiza root alleviates cerebral ischemia reperfusion injury by inhibiting oxidative stress induced apoptosis through PI3K/AKT/Bcl-2/Bax signaling pathway. *J. Ethnopharmacol.* **316**, 116698. https://doi.org/10.1016/j.jep.2023.116698 (2023).
53. Li, X. et al. Quantitative proteomics analysis reveals an important role of the transcriptional regulator UidR in the bacterial biofilm formation of Aeromonas hydrophila. *Front. Cell. Infect. Microbiol.* **14**, 1380747. https://doi.org/10.3389/fcimb.2024.1380747 (2024).
54. Liu, J. et al. Intestinal metabolomics in premature infants with late-onset sepsis. *Sci. Rep.* **14**, 4659. https://doi.org/10.1038/s41598-024-55398-7 (2024).
55. Guo, L. et al. Platelet MHC class I mediates CD8+ T-cell suppression during sepsis. *Blood* **138**, 401–416. https://doi.org/10.1182/blood.2020008958 (2021).
56. Cheng, L., Liu, D. & Gao, S. PPARA ameliorates sepsis-induced myocardial injury via promoting macrophage M2 polarization by interacting with DUSP1. *Regen. Ther.* **26**, 33–41. https://doi.org/10.1016/j.reth.2024.04.017 (2024).
57. Chaturvedi, V. et al. T-cell activation profiles distinguish hemophagocytic lymphohistiocytosis and early sepsis. *Blood* **137**, 2337–2346. https://doi.org/10.1182/blood.2020009499 (2021).
58. Ramljak, D. et al. Early response of CD8+ T cells in COVID-19 patients. *J. Pers. Med.* https://doi.org/10.3390/jpm11121291 (2021).
59. Graßhoff, H. et al. Low-dose IL-2 therapy in autoimmune and rheumatic diseases. *Front. Immunol.* **12**, 648408. https://doi.org/10.3389/fimmu.2021.648408 (2021).
60. Raeber, M. E., Sahin, D., Karakus, U. & Boyman, O. A systematic review of interleukin-2-based immunotherapies in clinical trials for cancer and autoimmune diseases. *EBioMedicine* **90**, 104539. https://doi.org/10.1016/j.ebiom.2023.104539 (2023).
61. Garonzi, C., Chinello, M. & Cesaro, S. Emapalumab for adult and pediatric patients with hemophagocytic lymphohistiocytosis. *Expert. Rev. Clin. Pharmacol.* **14**, 527–534. https://doi.org/10.1080/17512433.2021.1901576 (2021).

Acknowledgements
We thank our departmental colleagues for their assistance with this study. This study was supported by the Youth Top Talent fund of Chongqing Hospital of Traditional Chinese Medicine (CQSZYY2022007) .

Author contributions
LH designed the study; LH, LGS and TXX carried out the research and wrote the paper;TXX, LGS, WEY and ZH collected the samples; LGS and TXX performed the experiments; LGS and TXX acquired and analysed the data; LH revised the manuscript. LGS and TXX contributed equally to this work and should be considered as first authors. All authors read and approved the final manuscript.

Declarations

Conflict of interest
The authors declare no competing interests.

Ethical approval
Ethical approval for human sample usage was obtained from the Ethics Committee of Chongqing Hospital of Traditional Chinese Medicine (approval number: 2024-IIT-HY-4), and all participants provided written informed consent.

Additional information
Supplementary Information The online version contains supplementary material available at https://doi.org/10.1038/s41598-025-03282-3.

Correspondence and requests for materials should be addressed to H.L.

Reprints and permissions information is available at www.nature.com/reprints.

Publisher's note Springer Nature remains neutral with regard to jurisdictional claims in published maps and institutional affiliations.